

Supporting information for: High-throughput design of Na-Fe-Mn-O cathodes for Na-ion batteries

Shipeng Jia¹, Jonathan Counsell², Michel Adamič¹, Antranik Jonderian¹, and Eric McCalla^{1,}*

¹Department of Chemistry, McGill University, Montreal, Canada

²Kratos Analytical Ltd., Wharfside, Trafford Wharf Road, Manchester, United Kingdom

* Corresponding author: eric.mccalla@mcgill.ca

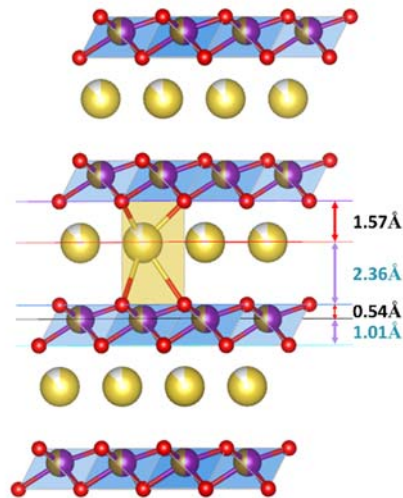


Figure S1: The structure of P3 determined from ref. S1. Of particular note here, there is a strong asymmetry in the vertical direction for the MO_6 polyhedra that is inconsistent with the symmetry in the stacking of the other layers. The z-direction as discussed in the main text is vertical in this image.

Phase Diagram of $\text{Na}_x\text{Fe}_y\text{Mn}_z\text{O}_n$

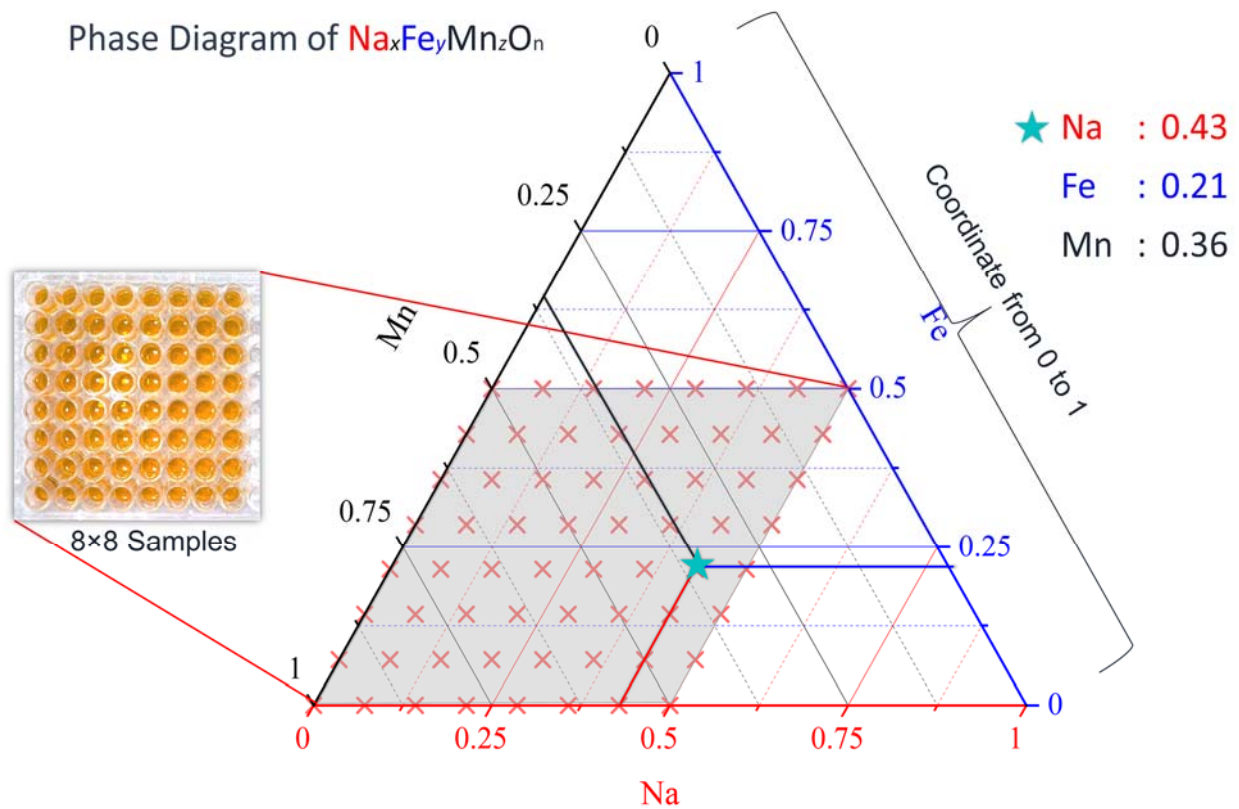


Figure S2: Illustration of how volume ratios are utilized to map out a ternary phase diagram using mixtures of equimolar solutions of the three corners.

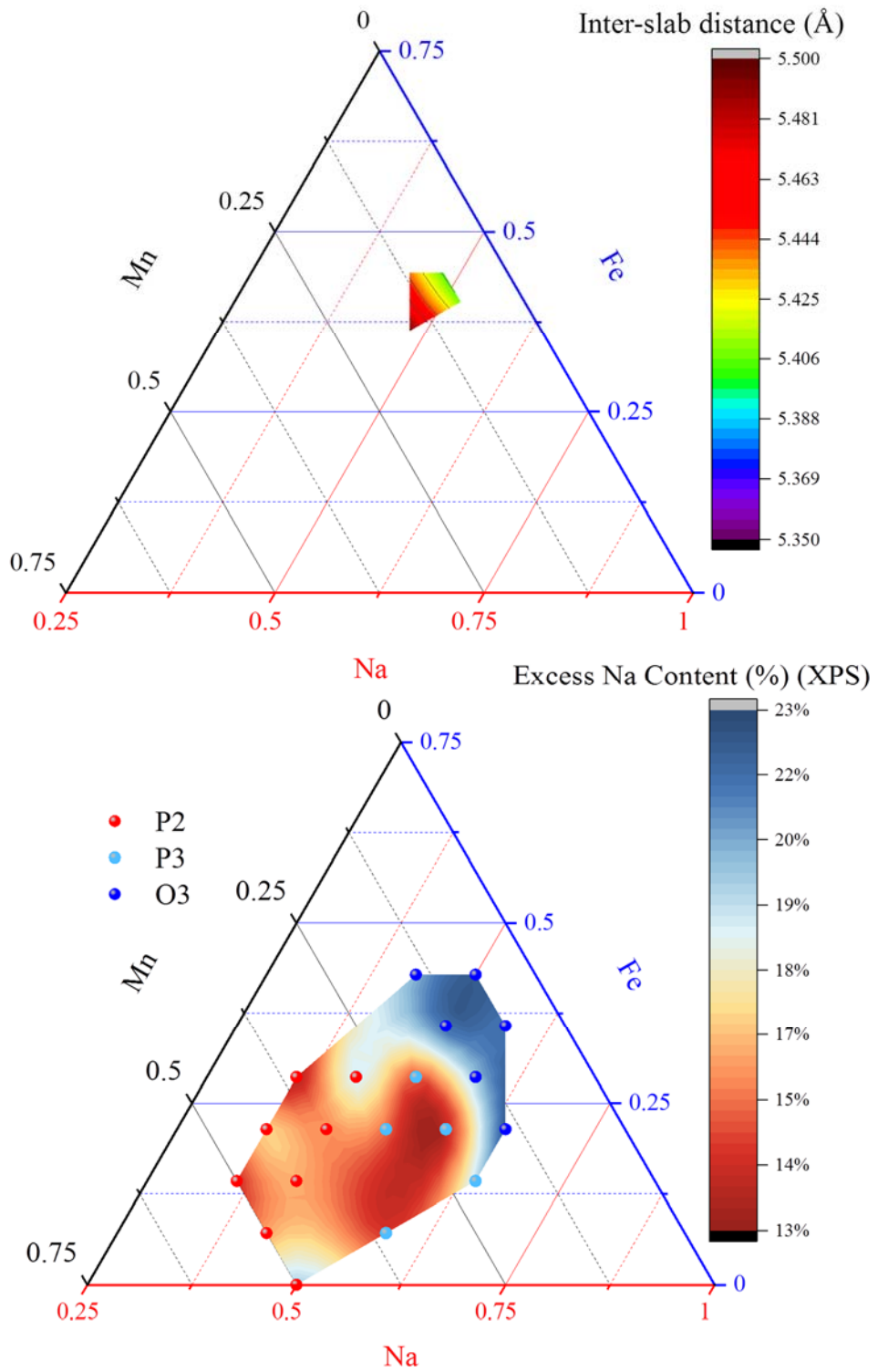


Figure S3: Top: inter-slab distance for the O3 phase only. Bottom: the excess Na content calculated from the XPS quantitative analysis.

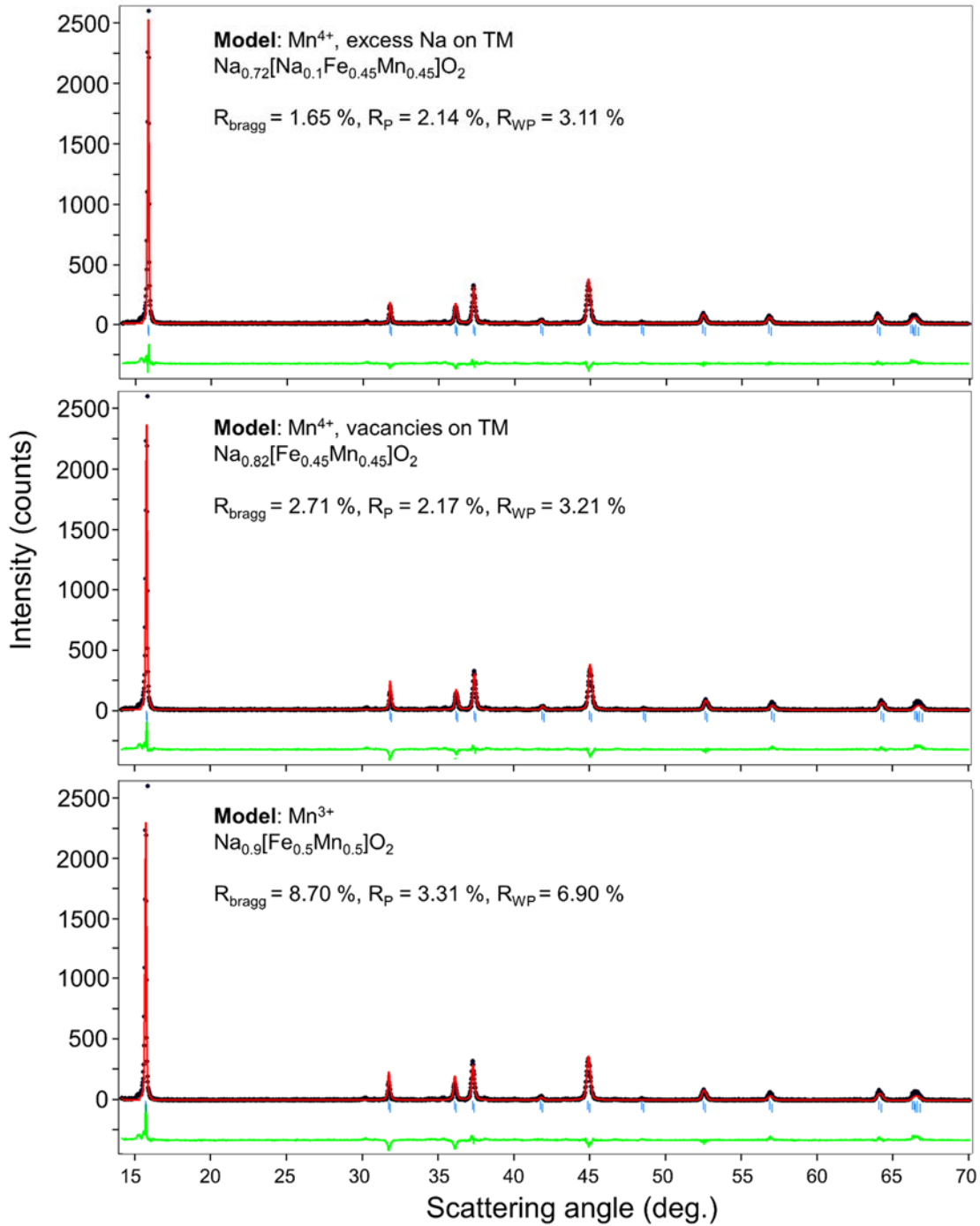


Figure S4: Three Rietveld fits for a P3 sample. The background has been subtracted for clarity.

Black: data, red: fit result, green: difference plot. The values of the fit quality parameters are shown for all 3 models discussed in the main text. The fits are undeniably improved when one considers Mn in the 4+ state, consistent with XAS results from ref. S1.

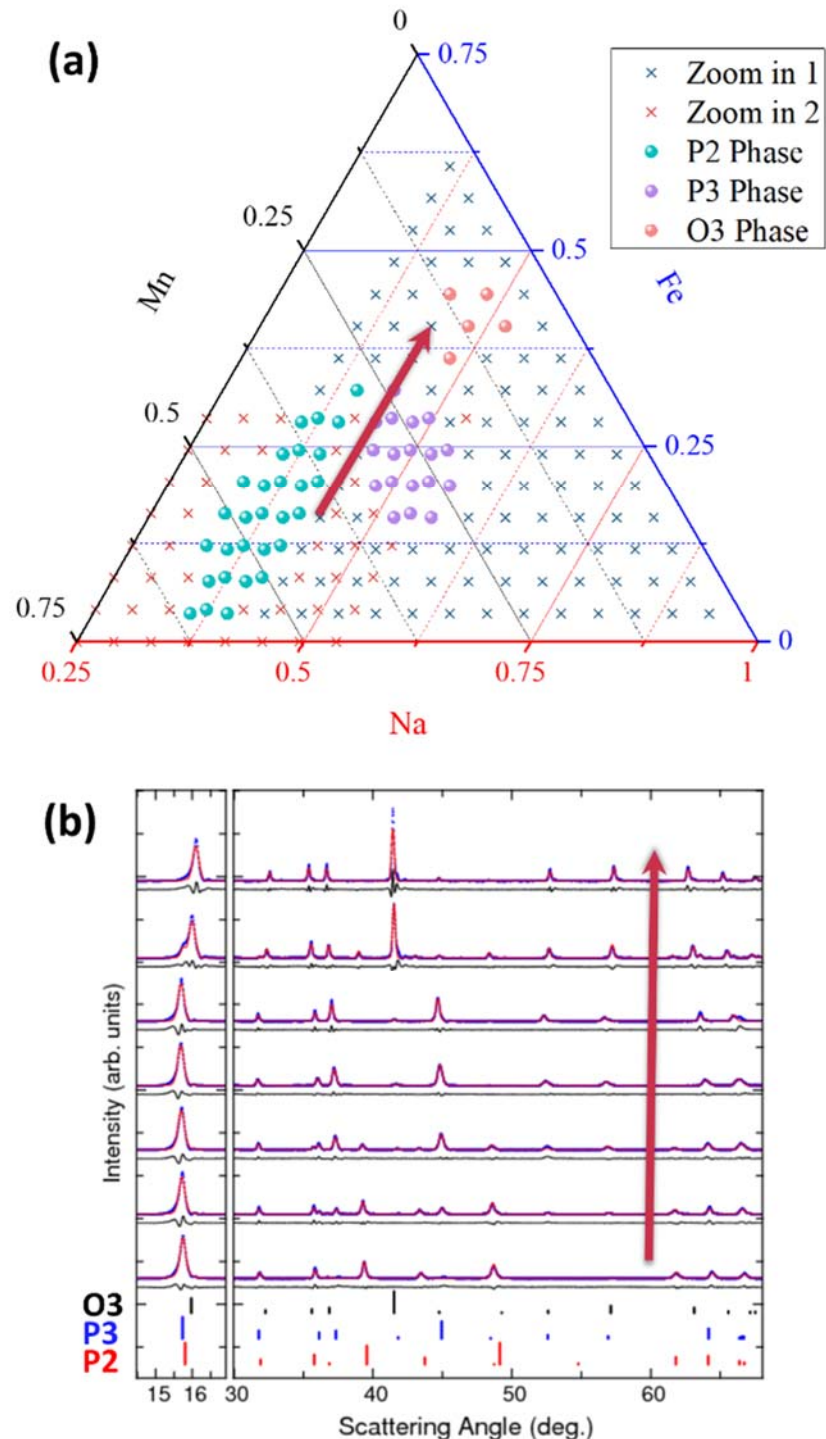


Figure S5: (a) Composition line through the phase diagram that shows a transition from P2 to P3 and then very near to the O3 region. (b) The corresponding XRD patterns, with fits in red, and difference plots below each pattern.

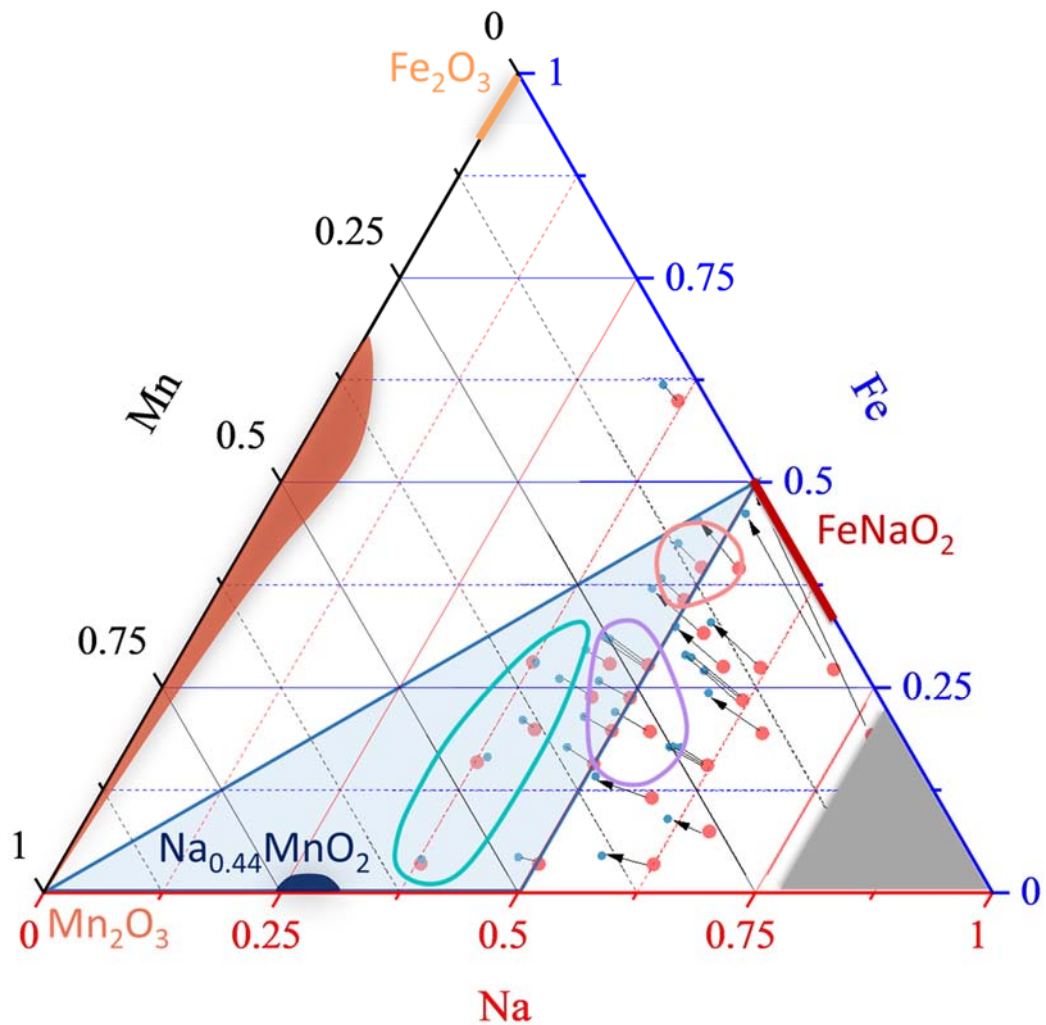


Figure S6: The phase stabilities determined herein along with the map of Na loss and the blue triangular region where layered oxides can form with Fe in the 3+ state, Mn taking a mixed 3,4+ state and no vacancies on the TM layers.

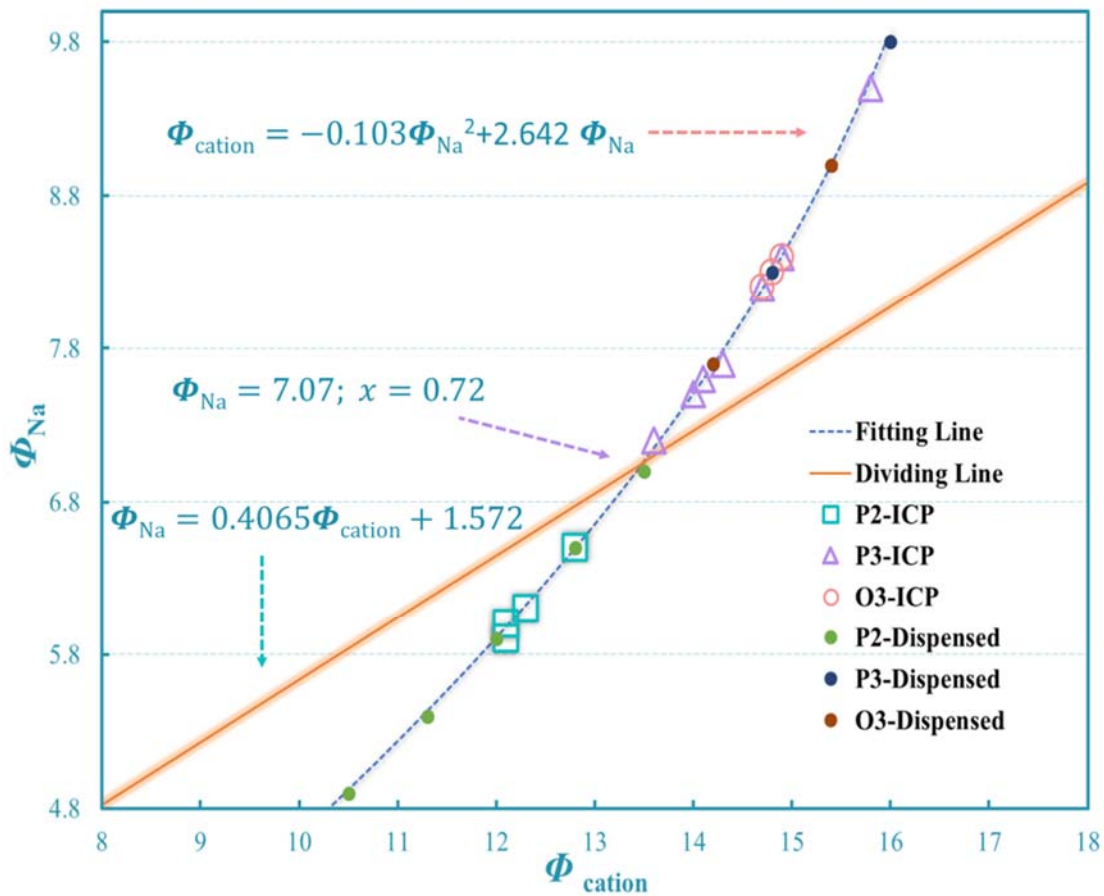


Figure S7: Result of the cationic potential analysis if Mn is assumed to be in a state such that Mn and Fe fully occupy the TM layers. As discussed throughout, this condition does not hold for the P3 structures based on our Rietveld refinement and XAS measurements from ref. S1.

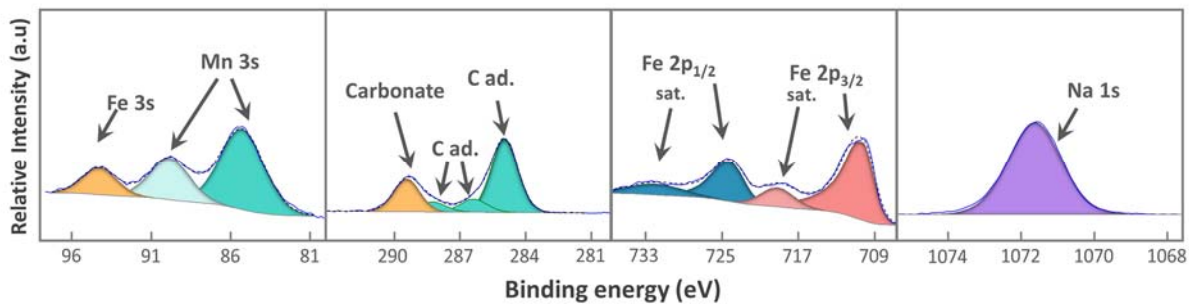


Figure S8: XPS of a single P2 sample. Peaks of Mn 3s, C 1s, Fe 2p, and Na 1s are labelled.

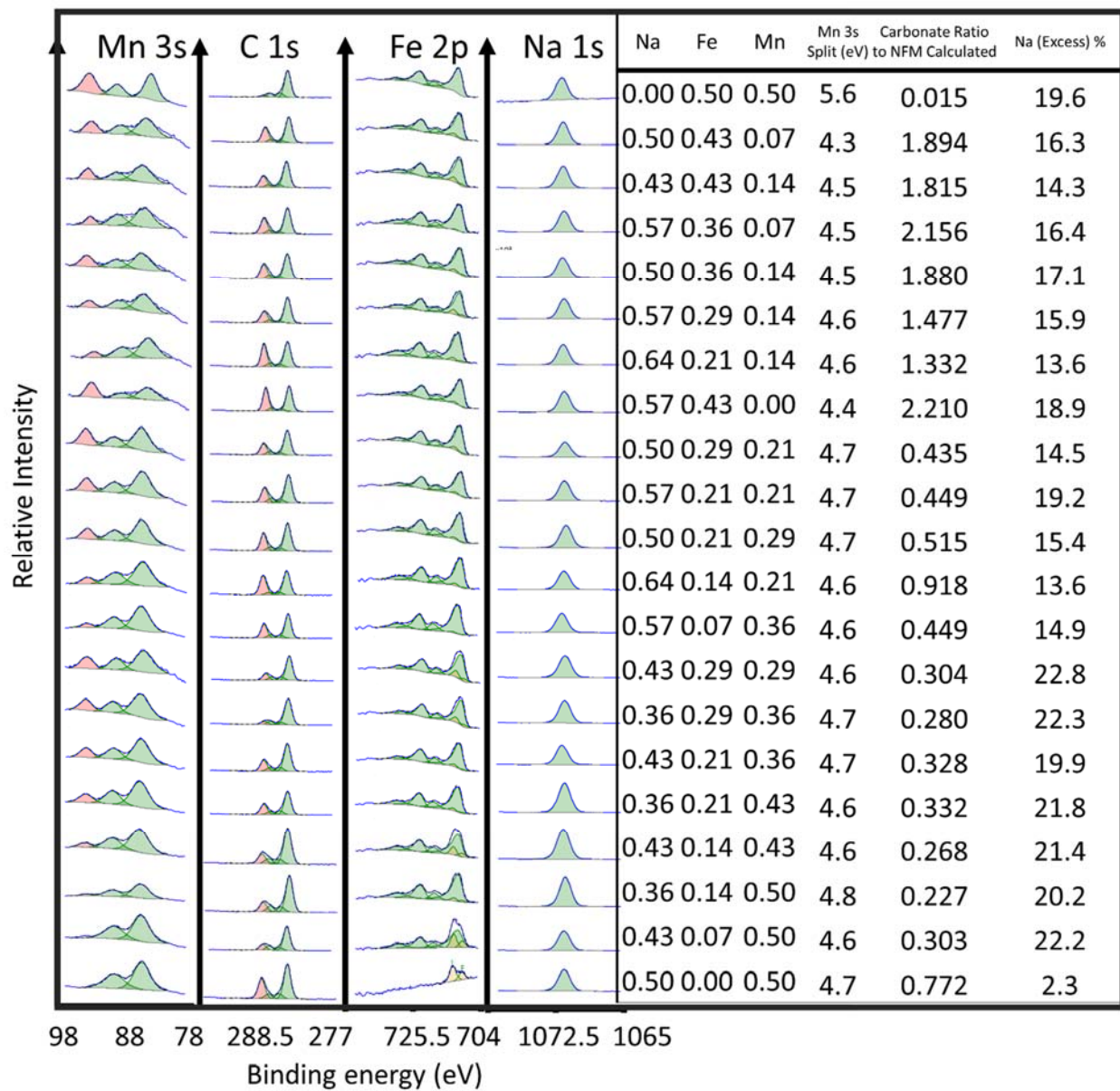


Figure S9: The complete set of XPS patterns, along with Na, Fe, Mn content, Mn 3s splitting and carbonate ratio.

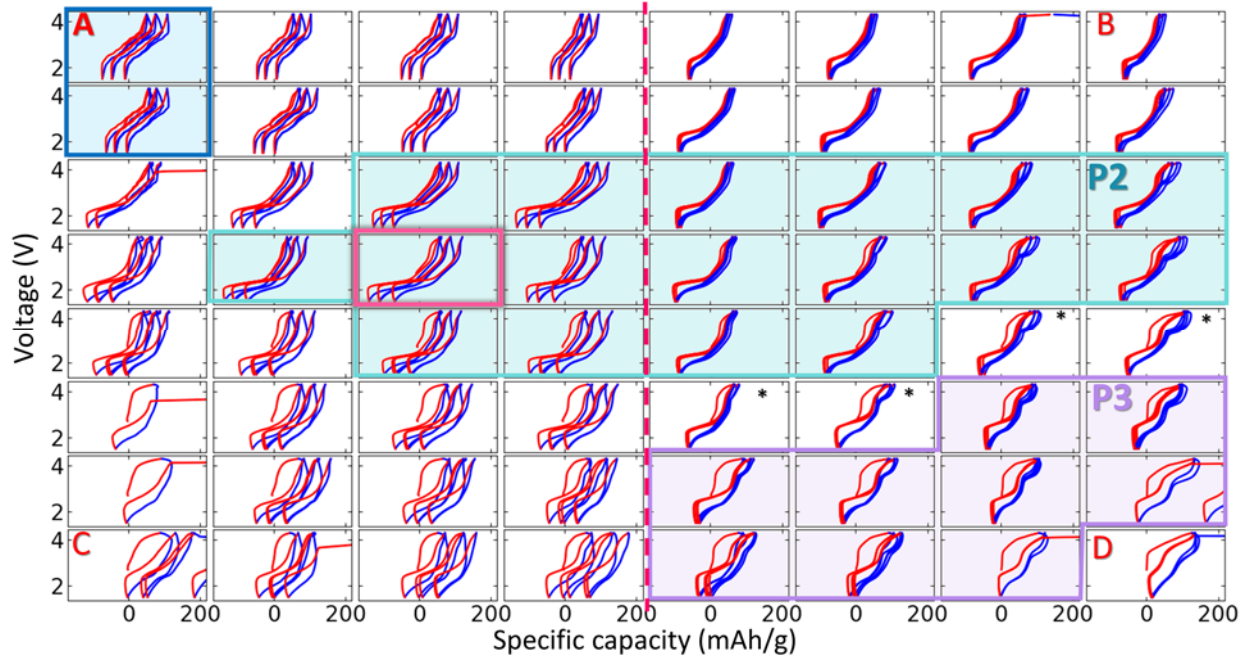


Figure S10: 5 cycles of zoom-in 2. The focus here is on charge endpoint slippage (the voltage curves drift to the right with extended cycling): the entire left half shows high slippage, while the right half shows greatly reduced slippage. The line between the two halves is an iron content of 16% as discussed in the main text.

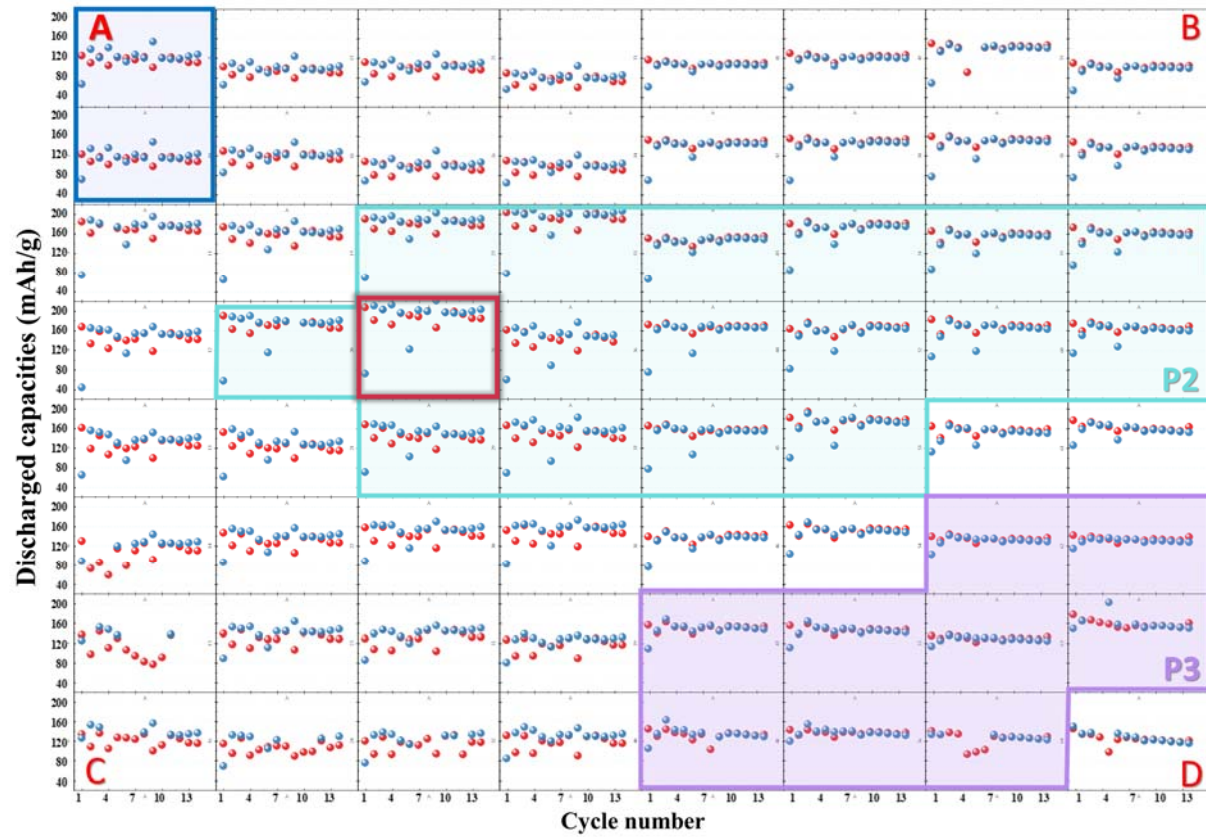


Figure S11: Specific capacity during charge (blue) and discharge (red) for 15 cycles for the materials made in zoom-in 2. The compositions at the four corners are indicated and match the labels on **Figure 2a**.

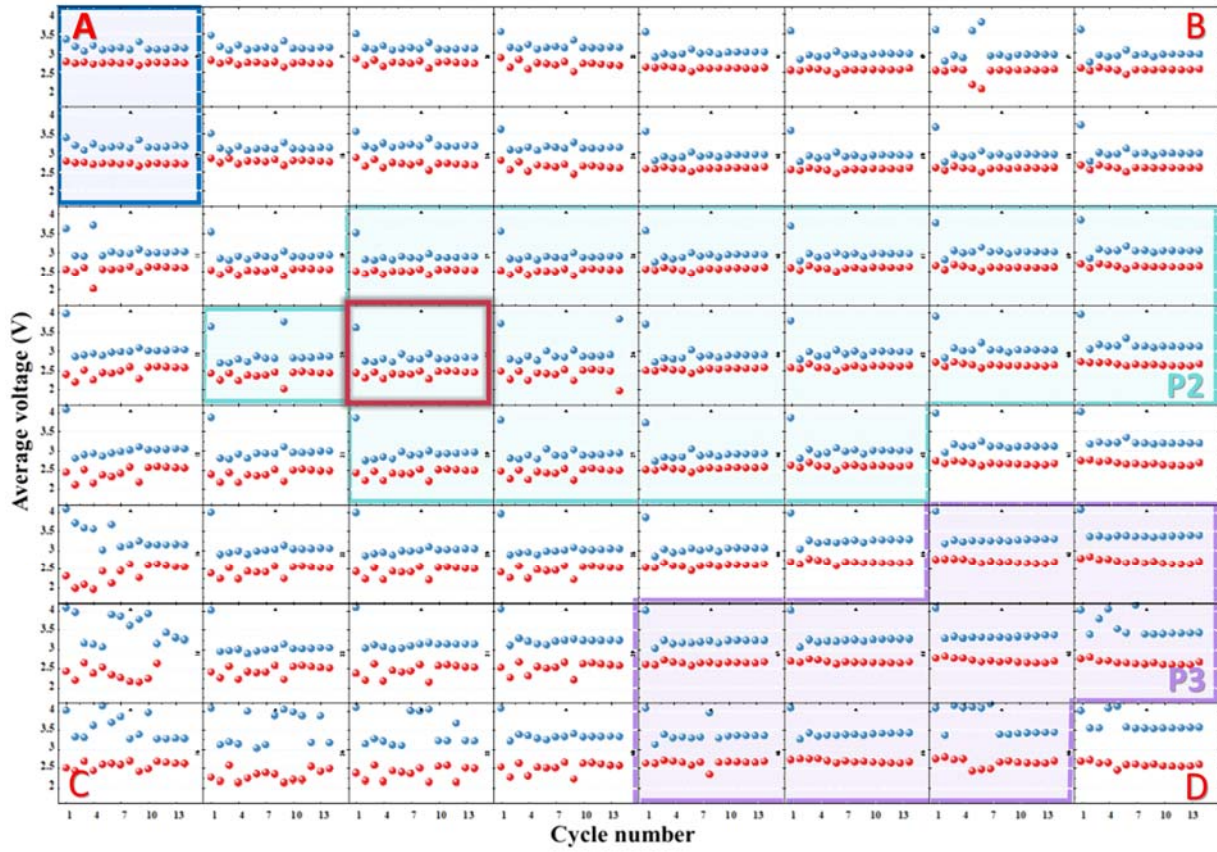


Figure S12: Average voltage during charge (blue) and discharge (red) for 15 cycles for the materials made in zoom-in 2.

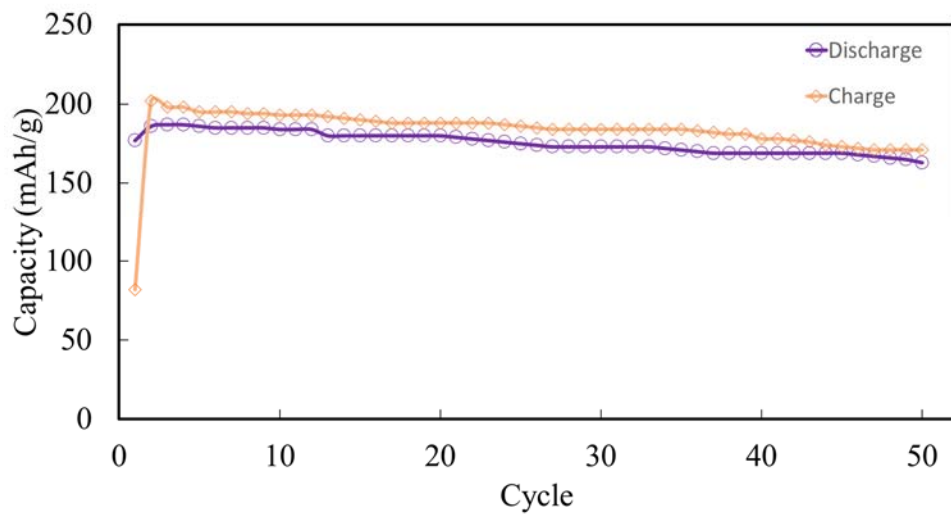


Figure S13: Specific capacity (orange is for charge, blue is for discharge) vs. cycle number for the highest capacity P2 material cycled in a Swagelok cell.

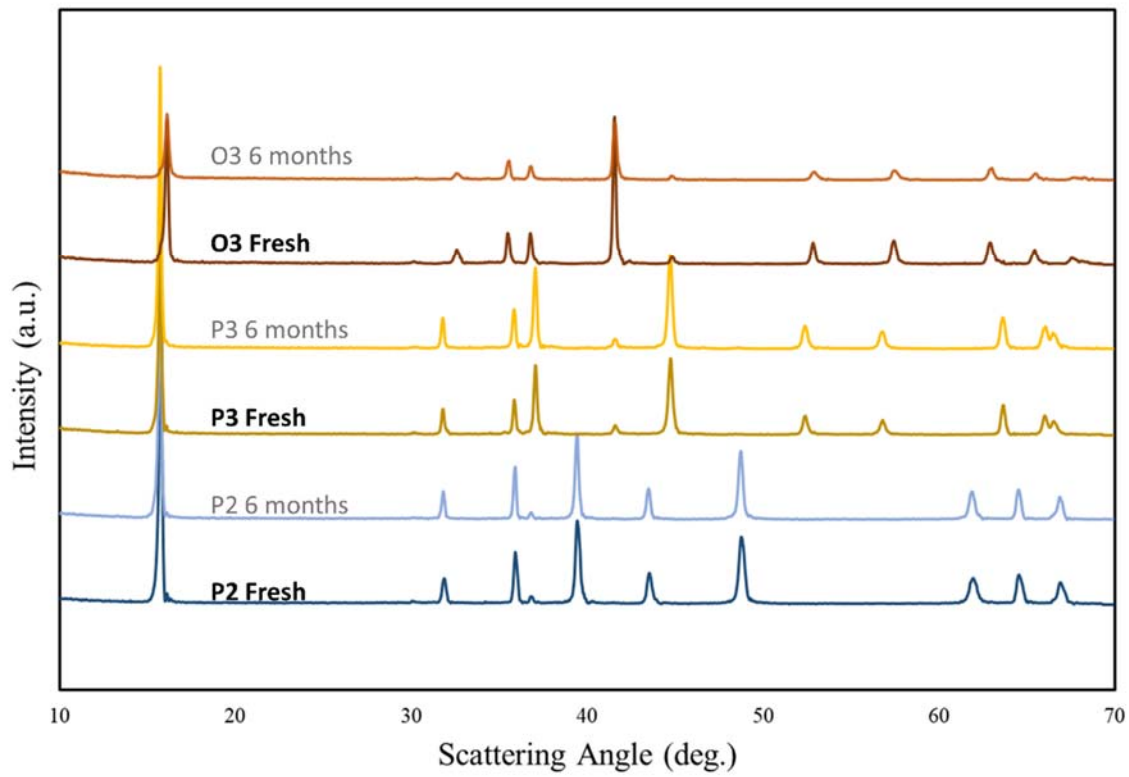


Figure S14. XRD results for air stability with as-prepared and after-6-month P2, P3, and O3 materials with the same compositions as used in Figure 10.

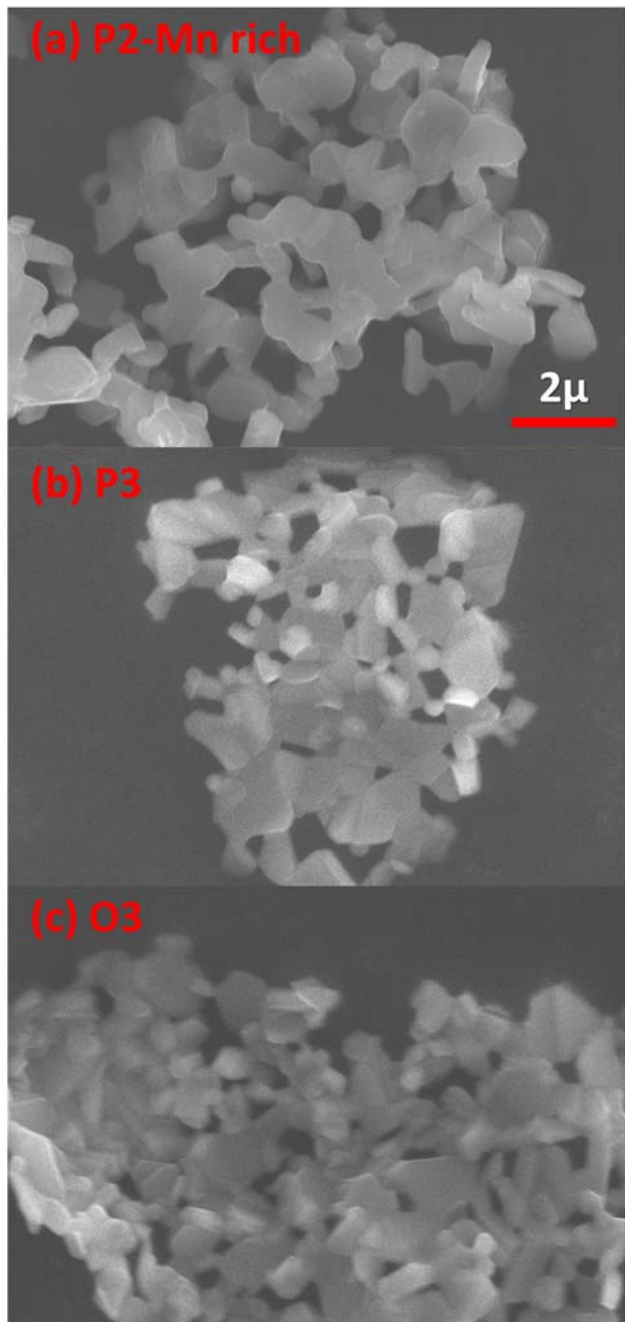


Figure S15. Representative SEM image for sol-gel combinatorial samples (a) P2-
 $\text{Na}_{0.59}\text{Fe}_{0.13}\text{Mn}_{0.87}\text{O}_2$, (b) P3- $\text{Na}_{0.74}\text{Fe}_{0.54}\text{Mn}_{0.41}\text{O}_2$, and (c) O3- $\text{Na}_{0.85}\text{Fe}_{0.70}\text{Mn}_{0.30}\text{O}_2$.

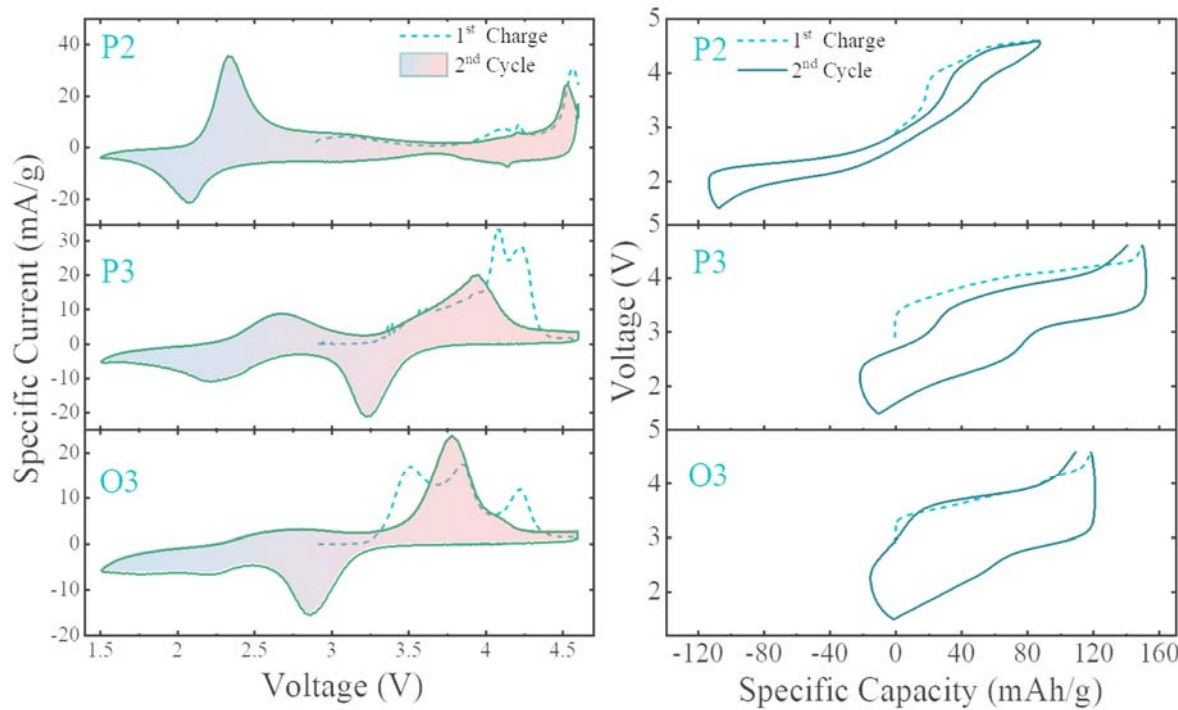


Figure S16. The first 1.5 cycles shown as both CVs (left) and voltage curves (right) from 1.5 V to 4.6 V at the scan rate 0.1 V/h for the P2, P3 and O3 materials showing highest first discharge capacities within their respective phases. Specifically, the compositions are: $\text{Na}_{0.59}\text{Fe}_{0.13}\text{Mn}_{0.87}\text{O}_2$ (P2), $\text{Na}_{0.74}\text{Fe}_{0.54}\text{Mn}_{0.41}\text{O}_2$ (P3), and $\text{Na}_{0.85}\text{Fe}_{0.70}\text{Mn}_{0.30}\text{O}_2$ (O3).

References

S1. A. Tripathi, S. Xi, S. R. Gajjela and P. Balaya, *Chemical Communications*, 2020, **56**, 10686-10689.